IEEE Photonics Journal
An IEEE Photonics Society Publication

Open Access

Dual-Wavelength Mid-Infrared Generation Using Intracavity Stimulated Raman Scattering of PPLN

Volume 10, Number 6, December 2018

Peng Wang
Xi Cheng
Xiao Li
Xiaojun Xu
Kai Han
Jian Chen

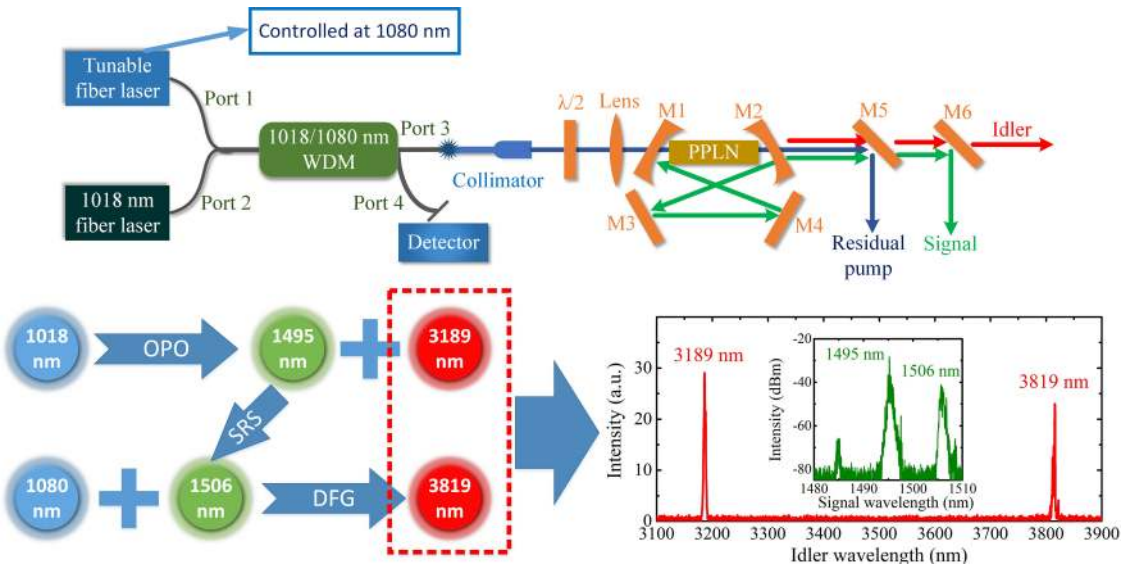

DOI: 10.1109/JPHOT.2018.2875709
1943-0655 © 2018 IEEE

IEEE photonics SOCIETY

IEEE

Dual-Wavelength Mid-Infrared Generation Using Intracavity Stimulated Raman Scattering of PPLN

Peng Wang,[1] **Xi Cheng**,[1] **Xiao Li**,[1] **Xiaojun Xu**,[1] **Kai Han**,[1] **and Jian Chen**[2]

[1]College of Advanced Interdisciplinary Studies, National University of Defense Technology, Changsha 410073, China
[2]Anhui Province Key Laboratory of Non-Destructive Evaluation, ZC Optoelectronic Technologies, Ltd., Hefei 230000, China

DOI:10.1109/JPHOT.2018.2875709
1943-0655 © 2018 IEEE. Translations and content mining are permitted for academic research only. Personal use is also permitted, but republication/redistribution requires IEEE permission. See http://www.ieee.org/publications_standards/publications/rights/index.html for more information.

Manuscript received September 9, 2018; revised September 26, 2018; accepted October 9, 2018. Date of publication October 12, 2018; date of current version October 29, 2018. This work was supported by Open Research Fund of State Key Laboratory of Pulsed Power Laser Technology, Electronic Countermeasure Institute, National University of Defense Technology (SKL2017KF04). Corresponding authors: Xiao Li and Xiaojun Xu (e-mail: crazy.li@163.com; xuxj@21cn.com).

Abstract: We report, to the best of our knowledge, the first demonstration of a continuous-wave, dual-wavelength (DW) mid-infrared optical parametric oscillator (OPO) based on the stimulated Raman scattering (SRS) effect of periodically poled lithium niobate (PPLN). The OPO was pumped by two independent fiber lasers, one being fixed at 1018 nm and the other being tunable. The high-power 1018-nm source built parametric oscillation, induced SRS effect in PPLN and generated 1495-nm signal beam as well as 1506-nm Raman beam. The tunable fiber laser was set at 1080 nm and the phase-matched difference frequency generation (DFG) occurred between the 1506-nm Raman beam and 1080-nm pump beam. Finally, DW idler beam located at 3189 and 3819 nm was obtained whose power ranged from 8.044 to 8.115 W, in which the 3189-nm idler power made up the majority of about 8 W and the maximum 3819-nm idler power reached 0.154 W. The slope and conversion efficiency of DFG and OPO processes was also discussed separately.

Index Terms: Infrared lasers, fiber lasers, nonlinear crystals, nonlinear.

1. Introduction

Because of containing important transparent window of the atmosphere and nearly all fundamental rovibrational absorption bands of molecules, the mid-infrared sources have been widely used in the areas of environment monitoring, medical diagnosis and counter-measurement [1]–[3]. In particular, DW mid-infrared sources are needed in some special applications including high-speed differential absorption lidar, chemical sensing and THz-wave generation [4]–[8]. Since the first actual OPO based on the $LiNbO_3$ crystal was demonstrated by Giordmaine and Miller in 1965 [9], they have become well-established mid-infrared sources which can offer coherent light, high power, broad bandwidth and tunable range. In the case of an OPO with a single resonator, mid-infrared DW operation has been realized via several approaches. Yuwei Jin *et al.* demonstrated a two-crystal mid-infrared DW OPO, which was realized by using two MgO:PPLN crystals in a ten-mirror resonant cavity [10]. V. Ramaiah-Badarla *et al.* reported a picosecond DW mid-infrared OPO which was also based on two MgO:PPLN crystals sharing the same cavity and synchronously pumped by a fiber

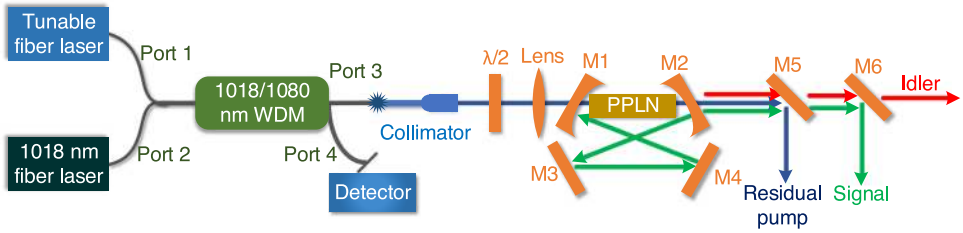

Fig. 1. Schematic diagram of CW DW OPO based on SRS effect of PPLN.

laser [11]. Peipei Jiang *et al.* demonstrated fiber laser pumped DW OPOs based on aperiodically poled MgO:LN wafers which had a special structure of aperiodic optical superlattice (AOS) [12], [13]. Compared with other kinds of pump sources, fiber lasers have the potential to achieve multi-wavelength output without complicate structure. In the previous work, we have obtained dual- and triple-wavelength mid-infrared output based on simultaneous intracavity OPO and DFG in single resonant cavity pumped by multi-wavelength fiber lasers [14], [15].

The SRS effect is a common third-order nonlinear effect and has been observed in many crystals. In 2006, the intracavity-pumped SRS operation in a fiber-laser-pumped CW MgO:PPLN OPO was observed for the first time by A. V. Okishev and J. D. Zuegel [16]. The 1st and 2nd stokes shift were calculated and they found that the SRS acted as a limiter to the intracavity signal power, increasing the idler output power stability. Angus Henderson and Ryan Stafford also observed the stimulated Raman conversion of the signal wave to Stokes and anti-Stokes bands [17]. It can be speculated that DW mid-infrared radiation can be obtained by injecting another pump beam into the cavity for inducing phase-matched DFG between it and the intracavity Raman beam. To prove this assumption, in this letter, we demonstrated DW mid-infrared generation using SRS effect of PPLN based on simultaneous OPO and DFG processes. Two independent fiber lasers were adopted as pump sources, one being fixed at 1018 nm and the other being tunable. The high-power 1018 nm source was used for building parametric oscillation and generating 1506 nm Raman beam while the tunable source was used for inducing DFG process between it and the Raman beam. The tunable source was set at 1080 nm to enable the DFG process satisfy phase-matching conditions. Finally, DW idler beam was obtained with central wavelengths located at 3189 nm and 3819 nm. The total idler power ranged from 8.044 W to 8.115 W, in which the 3189 nm idler power was around 8 W and the 3819 nm idler power increased from 15 mW to 0.154 W. The slope and conversion efficiency of the DFG process was calculated to be 6.72% and around 6%, much lower than the 1018 nm pumped OPO (>20%). Better results are expected to be realized by using temperature control and more precise pump wavelength tuning. This is, to the best of our knowledge, the first report on DW mid-infrared generation based on SRS effect of PPLN, which may be helpful for further studying SRS of PPLN and provide an effective approach to realize DW mid-infrared radiation.

2. Experiment Setup

Figure 1 illustrates the configuration of the fiber-laser-pumped CW DW OPO. The pump sources were two home-made CW linearly polarized fiber lasers. One fiber laser was fixed at 1018 nm and the other was tunable from 1060 nm to 1100 nm. The maximum power of them were 33.5 W (for 1018 nm laser) and 2.4 W (for tunable laser) separately. They were combined in parallel by a 1018/1080 nm polarization-maintaining (PM) wavelength division multiplexer (WDM) whose maximum power handing capacity was 40 W. As depicted in Fig. 1, two ports of the WDM, port 1 and port 2, were connected with two fiber lasers and the DW pump beam was outputted from port 3 while about a hundredth of the total power was outputted from port 4 for spectrum measurement to monitor working status of two fiber lasers. A fiber collimator was fused with port 3 and emitted the collimated DW pump beam whose spot size was measured to be 2 mm. The pump beam

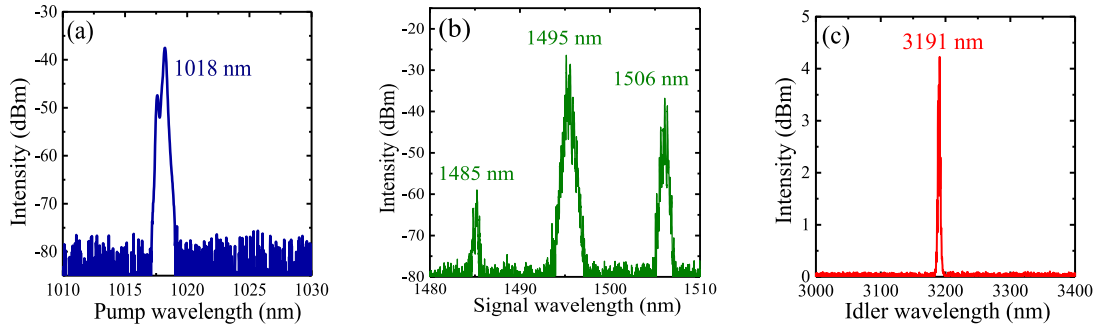

Fig. 2. Measured (a) pump, (b) signal and (c) idler spectra under 1018 nm pumping.

was incident into the resonant cavity and focused in the center of the crystal by passing through a focusing lens whose focal length was 150 mm. The radius of pump beam waist was measured to be about 80 μm. The OPO used a four-mirror ring cavity design, which consisted of two plane and two concave (radius of curvature $=$ 150 mm) CaF_2 mirrors, M1 to M4 shown in the figure. The curved mirrors, M1 and M2, were separated by 280 mm and the plane mirrors, M3 and M4, by 262 mm. The angle of incidence at each mirror was about 7°. Three mirrors, M1, M3 and M4, were dielectrically coated for high reflection for signal wavelengths (Rs $>$ 99.9% at 1400$\sim$1700 nm) and high transmission for the pump and idler wavelengths (Tp, Ti $>$ 95% at 1000$\sim$1100 nm and 2700$\sim$4000 nm). The output-coupling mirror, M2, were high transmissive for the pump and idler wavelengths, and partially transmissive (T$\sim$10%, non-optimized) for signal wavelengths. A 50 mm-long 5% MgO-doped PPLN (MgO:PPLN) was placed at the focal position between the two curved mirrors. The light pass surfaces of PPLN had the size of 1 mm $*$ 10 mm and was carefully polished. The PPLN used in this experiment had just one grating period at 29.84 μm. After the resonant cavity was a collimating lens enabling output beams parallel for accurate measurement and two dichroic mirrors, M5 and M6, which were used to separate residual pump, signal and idler beams. The OPO system has been integrated and moduled with the fiber collimator as shown in Ref. [18], which insured the reliability of experiment results under different pump conditions. No extra temperature controller was added in the experiment.

3. Experiment Results and Discussion

For confirming the wavelength of PPLN-based Raman laser, the OPO was firstly pumped by the 1018 nm fiber laser. The measured pump, signal and idler spectra at maximum pump power were shown in Fig. 2. The figures reveal that the 1018 nm pump beam had a full width at half maximum (FWHM) of 0.22 nm. The signal spectrum had three peaks, located at 1485 nm, 1495 nm and 1506 nm separately. The idler beam was located at 3191 nm. Obviously the 1495 nm radiation was signal beam generated by 1018 nm pump beam while the 1485 nm and 1506 nm radiation was the 1st anti-Stokes and Stokes Raman laser. The redshift and blueshift was 48 cm^{-1} and 45 cm^{-1} separately, roughly consistent with values measured in Refs. [16] and [17]. The peak value of 1485 nm and 1506 nm radiation was 33 dB and 11 dB (about 2000 times and 12.5 times) lower than the 1495 nm signal beam. It indicated that the 1485 nm Raman laser was not suitable for DW mid-infrared generation due to its extremely low power and just the 1506 nm Raman laser was suitable for this purpose. The FWHM of 1495 nm 1506 nm radiation was calculated to be 28 pm and 60 pm separately. Another phenomenon shown in Fig. 2(b) is that the signal spectrum was not a single frequency but showed a symmetric pattern of side modes, with a characteristic spacing that was observed to vary between 0.3 nm and 0.5 nm, which was similar to the result shown in Ref. [17]. It was analyzed that this was caused by high pump power as the Ref. [17] presented.

The maximum power of tunable fiber source was just 2.4 W, too low to build independent parametric oscillation for generating another idler beam. Then it was obvious that besides the 3191 nm

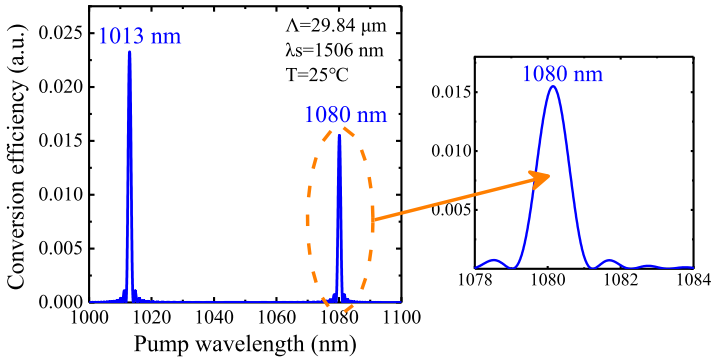

Fig. 3. Simulated DFG conversion efficiency versus the pump wavelength.

idle beam, the other idle beam should be generated based on the DFG between the tunable pump beam and 1506 nm Raman beam. For realizing the efficient DW mid-infrared generation, the DFG process should satisfy phase-matching conditions under the circumstances where the grating period was 29.84 μm and the temperature was 25 °C. According to the traditional theory, the DFG light field intensity and pump-to-idler conversion efficiency based on the small signal approximation can be written as following equations:

$$|I_i| = \frac{8\pi L^2 d_{eff}^2}{n_i n_p n_s \lambda_i^2 c\varepsilon_0} |I_p| |I_s| \left[\sin\left(-\frac{\Delta kL}{2}\right) \Big/ -\frac{\Delta kL}{2}\right]^2,$$

$$\eta_{DFG} = \frac{|I_i|}{|I_p|} = \frac{8\pi^2 L^2 d_{eff}^2}{n_i n_p n_s \lambda_i^2 c\varepsilon_0} |I_s| \left[\sin\left(-\frac{\Delta kL}{2}\right) \Big/ \left(-\frac{\Delta kL}{2}\right)\right]^2,$$

where L, d_{eff}, n_i, n_p, n_s, λ_i, c, ε_0 and I_s represent the PPLN length, effective nonlinear coefficient of PPLN, refractive index of idler, pump and signal beams in PPLN, idler wavelength, vacuum speed of light, vacuum permittivity and light field intensity of signal beam separately. The Δk represents the phase mismatch between pump, signal and idler waves after compensated by the PPLN and can be written as $\Delta k = 2\pi(n_p/\lambda_p - n_s/\lambda_s - n_i/\lambda_i - 1/\Lambda)$, in which Λ is the grating period of PPLN. It is obvious that after the 1018 nm pumped OPO reaches the steady state, the relationship in DFG can be obtained that is $\eta_{DFG} \propto (1/n_i n_p \lambda_i^2)[\sin(-\Delta kL/2)/(-\Delta kL/2)]^2$. According to the relationship, the simplified DFG conversion efficiency versus the wavelength of tunable fiber source was simulated and shown in Fig. 3. In the simulation, the grating period, PPLN temperature, the signal and pump wavelength was set as 29.84 μm, 25 °C, 1506 nm and ranging from 1000 nm to 1100 nm separately. The figure reveals that under these particular conditions, the conversion efficiency has two peaks where the corresponding pump wavelength was 1013 nm and 1080 nm, otherwise it is close to zero. The right picture was magnification of the conversion efficiency around 1080 nm. It reveals that the FWHM of conversion efficiency was about 1.1 nm. The tunable fiber source used in the experiment had a tuning range from 1060 nm to 1100 nm and could not reach 1013 nm. Thus, in order to achieve efficient DFG using 1506 nm Raman laser, the tunable fiber source should be set at 1080 nm.

According to the simulation result, the tunable fiber source was set at 1080 nm and the measured DW pump spectrum at maximum power was shown in Fig. 4. The figure reveals that the pump beam had two central wavelengths located at 1018 nm and 1080 nm. To be precise, the longer pump wavelength was 1080.3 nm, not exactly 1080 nm due to the inaccuracy of manual adjustment of tunable fiber laser but in the paper, it was written as 1080 nm for short. The FWHM of 1018 nm pump beam was still 0.22 nm while the FWHM of 1080 nm pump beam was 0.16 nm. The DW pump beam was incident into the resonant cavity and two nonlinear processes occurred. The signal and idler spectra under minimum and maximum 1080 nm pump power were measured and shown in

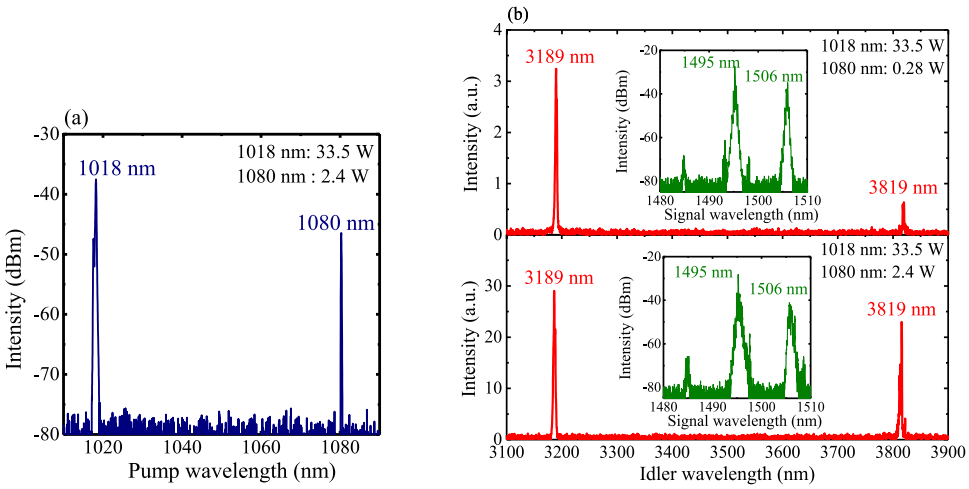

Fig. 4. (a) Measured DW pump spectrum at maximum pump power. (b) Measured signal and idler spectra under different 1080 nm pump power.

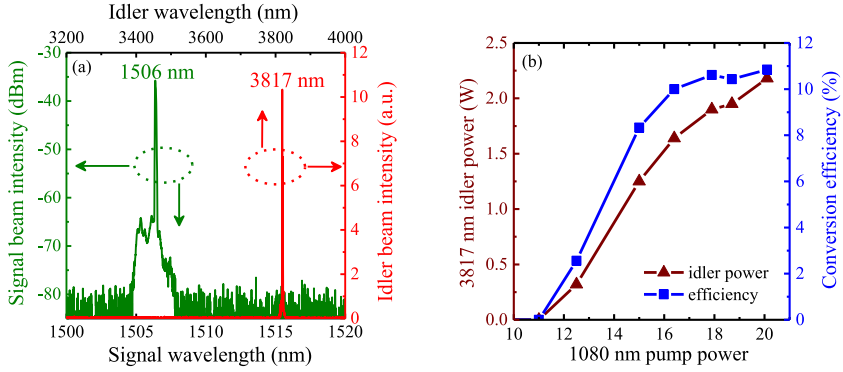

Fig. 5. Measured (a) signal and idler spectra, and (b) idler power and conversion efficiency when the OPO was pumped by single 1080 nm fiber laser.

Fig. 4(b). The figure reveals that no matter how large the 1080 nm pump power was, there always existed two idler beams located at 3189 nm and 3819 nm, indicating a 630 nm wavelength interval. The signal beam and 1st stokes laser was still fixed at 1495 nm and 1506 nm separately. Obviously the low-power 1080 nm pump beam was successfully transformed into 3819 nm idler beam based on the phase-matched DFG process between it and the 1506 nm Raman beam. The FWHM of 1495 nm and 1506 nm radiation was 70 pm and 80 pm separately. The signal and idler spectra didn't show apparent wavelength shift because the 1080 nm pump power as well as 3819 nm idler power (shown in the last paragraph) was relatively low and didn't raise additional heavy thermal effect in PPLN crystal.

For confirming the DFG process was phase-matched, the OPO was directly pumped by a 20 W 1080 nm fiber laser with the FWHM of 0.6 nm after the experiment finished. The measured signal and idler spectra was shown in Fig. 5(a). The figure reveals that the signal and idler beam was located at 1506 nm and 3817 nm separately, and the FWHM of signal beam was 70 pm. The result verified that although the pump wavelength in DFG process was a little longer than 1080 nm, the phase-matching conditions were satisfied because the parametric gain bandwidth of DFG was large enough for enabling 1080.3 nm pump beam realize efficient parametric conversion. The power characteristics of 1080 nm pumped OPO was shown in Fig. 5(b). As can be seen, the threshold

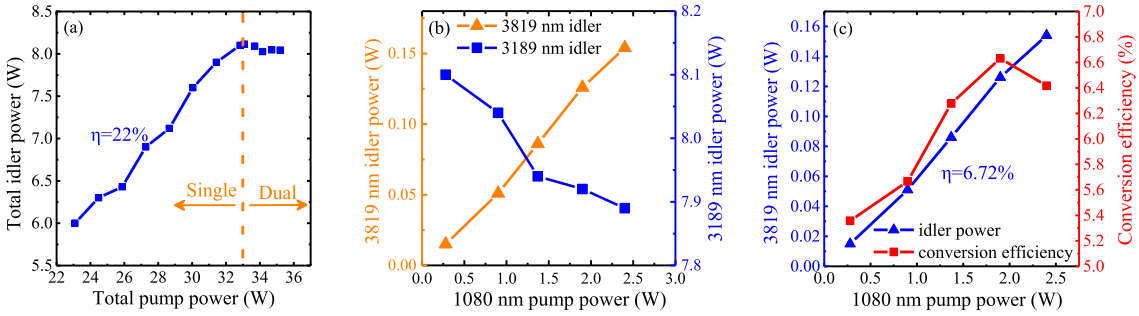

Fig. 6. (a) Measured total idler power versus total pump power. (b) Measured 3819 nm and 3189 nm idler power versus the 1080 nm pump power. (c) Measured 3819 nm idler power and pump-to-idler conversion efficiency versus the 1080 nm pump power.

for 1080 nm pumped OPO was about 11 W and the maximum idler power reached 2.18 W under 20 W pump power. The slope efficiency was about 22% and the conversion efficiency increased from almost zero to 11%.

The DW idler power as the function of the total DW pump power was measured and shown in Fig. 6(a). The figure reveals that before the 1080 nm pump beam joined in the parametric process, just the 3189 nm idler beam existed, and its power increased from 6 W to 8.1 W when the total pump power (1018 nm pump power) raised from 23 W to 33 W, indicating a 22% pump-to-idler slope efficiency. The conversion efficiency also can be calculated that was around 25%. After the 1080 nm pump beam was incident into the cavity, the DW idler power gradually decreased from 8.115 W to 8.044 W when the DW pump power increased from 33 W to 35.4 W. The 3189 nm and 3819 nm idler beams were divided using a mid-infrared dichroic mirror and their power versus the 1080 nm pump power was described in Fig. 6(b). The figure reveals that when the 1080 nm pump power increased from 0.28 W to 2.4 W, the 3819 nm idler power linearly increased from 15 mW to 0.154 W while the 3189 nm idler power decreased from 8.1 W to 7.89 W. Since the experiment setup and phase-matching conditions of 1018 nm pumped OPO didn't change, the decrease of 3189 nm idler power revealed that the 1495 nm signal power inside the resonant cavity decreased with increase of 1080 nm pump power. Moreover, the 1506 nm Raman power increased with 1080 nm pump power because the DFG consumed the 1080 nm pump power and transformed it to 3819 nm idler power and 1506 nm Raman power. Thus, it comes to the conclusion that increase of 1506 nm Raman power caused decrease of 1495 nm signal power as well as 3189 nm idler power. It can be speculated that when 1506 nm Raman beam became stronger, it increased 1st Raman gain and "attracted" more 1495 nm laser photons to transform to Raman laser photons. However, it was the speculation and needed further research. In the next study, a 1080 nm fiber laser with higher power will be used to replace the tunable fiber laser to research the impact on output characteristics of OPO caused by the DFG process. Fig. 6(c) depicts the 3819 nm idler power as well as pump-to-idler conversion efficiency versus the 1080 nm pump power. The slope efficiency of the DFG process was 6.72% and the conversion efficiency reached the maximum of 6.63% at 1.9 W pump power. Both of them were much lower than the 1018 m pumped OPO and 1080 nm pumped OPO. It was analyzed that the 1506 nm Raman beam was much lower than the 1495 nm signal beam, surely resulting in lower efficiency. Besides, not all Raman beam participated in DFG because part of it propagated backwards. In addition to these, the phase-matching conditions were not perfectly satisfied in the DFG process, also resulting in the low efficiency. Another phenomenon shown in Fig. 6(c) was that when the 1080 nm pump power increased from 1.9 W to 2.4 W, the DFG conversion efficiency exhibited slight decrease from 6.63% to 6.41%. It was analyzed that at the same power, the 3819 nm idler beam will cause higher thermal effect than the 3189 nm idler beam due to transmittance change of PPLN at different wavelength [19]. In the experiment when the 1080 nm pump power increased from 1.9 W to 2.4 W, the 3819 nm idler power increased by 0.03 W while the 3189 nm idle power decreased by 0.03 W. The slight

thermal effect was caused by 3819 nm idler beam and resulted in signal wavelength shift. However, the 1080 nm pump wavelength remained unchanged. The phase mismatch of DFG would increase and resulted in decrease of conversion efficiency. After all, the thermal effect was relatively small due to low 3819 nm idler power. Thus, the wavelength shift caused by thermal effect was small and didn't appear in the spectra shown in Fig. 4(b). Besides, the decrease of conversion efficiency was also relatively small. In the next research, temperature control of PPLN crystal and more accuracy tunable laser will be adopted for better DW mid-infrared generation.

4. Conclusion

In conclusion, for the first time, we demonstrated CW, DW mid-infrared generation using the SRS effect of PPLN in a mid-infrared OPO. The OPO was synchronously pumped by a 1018 nm fiber laser and a tunable fiber laser with the maximum power of 33.5 W and 2.4 W separately. The 1018 nm fiber laser built parametric oscillation and generated 1495 nm signal beam as well as 1506 nm Raman beam and the tunable fiber laser was used to generate mid-infrared radiation based on DFG between it and the 1506 nm Raman beam. For efficient DW generation, the tunable fiber laser was set at 1080 nm based on the DFG theory for satisfying phase-matching conditions. Ultimately, DW idler beam was obtained located at 3189 nm and 3819 nm separately. The total DW idler power ranged from 8.044 to 8.115 W, in which the 3189 nm idler power was around 8 W and the 3819 nm idler power ranged from 15 mW to 0.154 W. The slope efficiency and conversion efficiency of the DFG process was 6.72% and around 6%, much lower than the OPO process ($>$20%). Next research will be focused on more efficient and tunable DW mid-infrared generation by using temperature control and more precise pump wavelength adjusting.

Acknowledgment

The authors would like to thank Nanjing University, Zhejiang University, and Fujian Institute of Research on the Structure for their offer of nonlinear crystals.

References

[1] K. P. Petrov, L. Goldberg, W. K. Burns, R. F. Curl, and F. K. Tittel, "Detection of CO in air by diode-pumped 4.6-μm difference-frequency generation in quasi-phase-matched $LiNbO_3$," *Opt. Lett.*, vol. 21, no. 1, pp. 86–88, 1996.
[2] U. Willer, M. Saraji, A. Khorsandi, P. Geiser, and W. Schade, "Near- and mid-infrared laser monitoring of industrial processes, environment and security applications," *Opt. Laser Eng.*, vol. 44, no. 7, pp. 699–710, 2006.
[3] H. H. P. T. Bekman, J. C. van den Heuvel, F. J. M. van Putten, and R. Schleijpen, "Development of a midinfrared laser for study of infrared countermeasures techniques," *Proc. SPIE*, vol. 5615, pp. 27–38, 2004.
[4] M. S. Webb, K. A. Stanion, D. J. Deane, W. M. Cook, W. A. Neuman, and S. P. Velsko, "Multiwavelength injection-seeded midinfrared optical parametric oscillator for DIAL," *Proc. SPIE*, vol. 2700, pp. 269–300, 1996.
[5] A. R. Geiger, E. V. Degtiarev, W. H. Farr, and R. D. Richmond, "Mid-infrared multiwavelength source for lidar applications," *Proc. SPIE*, vol. 3380, pp. 63–69, 1998.
[6] Y. Jin, S. M. Cristescu, F. J. M. Harren, and J. Mandon, "Two-crystal mid-infrared optical parametric oscillator for absorption and dispersion dual-comb spectroscopy," *Opt. Lett.*, vol. 39, no. 11, pp. 3270–3273, 2014.
[7] K. Kawase, T. Hatanaka, H. Takahashi, K. Nakamura, T. Taniuchi, and H. Ito, "Tunable terahertz-wave generation from DAST crystal by dual signal-wave parametric oscillation of periodically poled lithium niobate," *Opt. Lett.*, vol. 25, no. 23, pp. 1714–1716, 2000.
[8] A. E. Klingbeil, J. B. Jeffries, D. F. Davidson, and R. K. Hanson, "Two-wavelength mid-IR diagnostic for temperature and n-dodecane concentration in an aerosol shock tube," *Appl. Phys. B*, vol. 93, pp. 627–638, 2008.
[9] J. A. Giordmaine and R. C. Miller, "Tunable coherent parametric oscillation in LiNbat optical frequencies," *Phys. Rev. Lett.*, vol. 14, no. 24, pp. 973–976, 1965.
[10] Y. Jin, S. M. Cristescu, F. J. M. Harren, and J. Mandon, "Broadly, independent-tunable, dual-wavelength mid-infrared ultrafast optical parametric oscillator," *Opt. Exp.*, vol. 23, no. 16, pp. 20418–20427, 2015.
[11] V. Ramaiah-Badarla, S. C. Kumar, and M. Ebrahim-Zadeh, "Fiber-laser-pumped, dual-wavelength, picosecond optical parametric oscillator," *Opt. Lett.*, vol. 39, no. 9, pp. 2739–2742, 2014.
[12] P. Jiang, T. Chen, D. Yang, B. Wu, S. Cai, and Y. Shen, "A fiber laser pumped dual-wavelength mid-infrared optical parametric oscillator based on aperiodically poled magnesium oxide doped lithium niobate," *Laser Phys. Lett.*, vol. 10, no. 11, pp. 1–4, 2013.
[13] S. Cai, J. Su, P. Wu, C. Hu, and P. Jiang, "Compact tunable dual-wavelength mid-infrared optical parametric oscillator pumped by high power gain-switched fiber laser," *Laser Phys. Lett.*, vol. 12, no. 7, 2015, Art. no. 075401.

[14] Y. Shang, P. Wang, X. Li, M. Shen, and X. Xu, "Frequency down-conversion of a dual-wavelength fiber laser," *Optik*, vol. 127, no. 24, pp. 11871–11876, 2016.
[15] P. Wang, Y. Shang, X. Li, M. Shen, and X. Xu, "Multi-wavelength mid-infrared laser generation based on optical parametric oscillation and intracavity difference frequency generation," *IEEE Photon. J.*, vol. 9, no. 1, Feb. 2017, Art. no. 150007.
[16] A. V. Okishev and J. D. Zuegel, "Intracavity-pumped raman laser action in a Mid-IR, continuous-wave (cw) MgO: PPLN optical parametric oscillator," *Opt. Exp.*, vol. 14, no. 25, pp. 12169–12173, 2006.
[17] A. Henderson and R. Stafford, "Spectral broadening and stimulated Raman conversion in a continuous-wave optical parametric oscillator," *Opt. Lett.*, vol. 32, no. 10, pp. 1281–1283, 2007.
[18] Y. Shang, J. Xu, P. Wang, X. Li, P. Zhou, and X. Xu, "Ultra-stable high-power mid-infrared optical parametric oscillator pumped by a super-fluorescent fiber source," *Opt. Exp.*, vol. 24, no. 19, pp. 21684–21692, 2016.
[19] M. Vainio, J. Peltola, S. Persijn, F. J. M. Harren, and L. Halonen, "Thermal effects in singly resonant continuous-wave optical parametric oscillator," *Appl. Phys. B*, vol. 94, no. 3, pp. 411–427, 2009.